

Convective near-wall flow in thermally stratified hot water storage tanks

Henning Otto*, Christian Resagk, Christian Cierpka

Technische Universität Ilmenau, Institute of Thermodynamics and Fluid Mechanics, Ilmenau, Germany

* henning.otto@tu-ilmenau.de

Abstract

Thermal energy storage systems (TES) are a major component of systems for the use of solar or industrial waste heat or can be used to store surplus energy from renewable power plants. Modern stratified TES use the thermal density gradient of the working fluid to produce a stable stratification of hot over cold fluid. Water is one of the most frequently used working fluids and generally enables a high thermal efficiency and thus long-term storage of thermal energy in such stratified TES. The walls of most TES consist of materials whose thermal diffusivity is significantly higher than this of water. Therefore the storage wall forms a thermal bridge between the hot and cold layer of water which leads to thermal convection inside the TES. This effect has the potential to disturb the stratification due to unwanted mixing of the two layers and thus decrease the overall efficiency of the storage system. A model experiment of a stratified TES was built and the impact of a heat conducting wall on the stratifications was shown by temperature measurements with and without this wall. Particle Image Velocimetry (PIV) measurements in the boundary layer of this wall were performed at different heights with a resolution of 62 px mm^{-1} . The results show two thin thermal convection flows close to the wall, one from top to bottom in the upper part of the experiment and the other from bottom to top in the lower part. These two flows approach in the middle of the thermocline and get redirected in a horizontal direction. The evaluation of time series data showed that the flow structures in the bottom and the middle region of the experiment are temporally constant and show only minor fluctuations. In the upper, hot area, the flow is subject to large fluctuations over the entire time. The investigations have demonstrated parasitic thermal convection inside stratified TES, which is associated with the formation of vortices, especially in the upper region, and can therefore strongly affect the stratification.

1 Introduction

Due to the global warming the German government has decided to promote an energy transition. The four main goals of this energy transition are to increase the fraction of renewable energy sources of the overall energy generation in Germany, to turn off the remaining nuclear power plants until 2022 and to decrease both the greenhouse emissions and the consumption of primary energy. To achieve these goals there is no other way than replacing coal and nuclear power plants with renewable energy sources. Wind turbines and solar power stations are two of the most used renewable energy sources but they have the disadvantage that they cannot generate energy on request. This circumstance leads to the fact that an energy transition is not possible without energy storage technologies which are capable to store large amounts of energy in an efficient and cost-effective way.

Thermal energy storages systems (TES) are one promising possibility to solve this problem. Besides batteries, compressed air energy storages or other storage concepts this storage system has the advantage of low investment costs and location independence. Combined with heat pump cycles electric energy can be converted to thermal energy which is stored in the TES [Thess (2013)]. On request a power cycle converts the thermal energy back to electricity. Through this type of use, the overall efficiency of TES as a storage system for electrical energy can be increased. Common TES in their simplest design are made of steel tanks filled with water, which works as storage medium. Both steel and water are easy accessible, relatively cheap and non-toxic raw materials in comparison to those which are need e.g. for electric battery storage systems.

The most effective way to use TES over a broad range of temperatures is to stratify the storage medium due to its temperature dependent density differences as can be seen in figure 5. This enables the direct use of the hot water during the discharging process. While the TES gets charged, heated water is filled into the

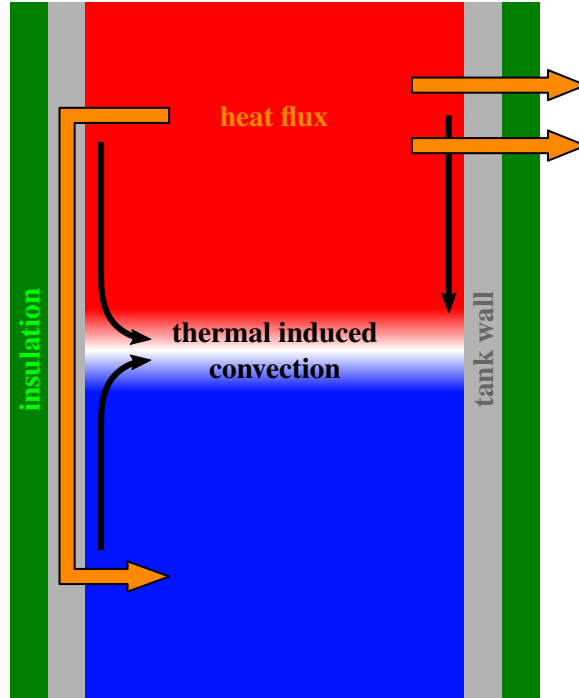


Figure 1: Depiction of the heat transfer processes inside a TES during standby phases. On the left side the heat flux from the hot to the cold region of a stratified storage medium through a tank wall with high thermal diffusivity is shown. On the right side the heat loss to the environment is shown. Both heat transfers induce thermal convection inside the storage medium.

upper part of the tank, where it maintains above the denser, cold water in the bottom. With its low thermal diffusivity of $a_w \approx 0.14 \cdot 10^{-6} \text{ m}^2 \text{ s}^{-1}$ and its high heat capacity of $4.18 \text{ kJ kg}^{-1} \text{ K}^{-1}$ water allows in general long term storing of thermal energy without convective mixing of hot and cold layers.

This general benefit of water as a storage medium is limited due to heat transfer processes which take place in TES. These heat transfers lead to a cooling or heating of the storage medium. As a result thermal convection is caused inside TES which may decrease the overall efficiency of the storage because of a mixing of the stratified storage medium.

In figure 1 two effects for induced thermal convection are shown. On the right side the heat loss of the TES to the environment is depicted. This effect cannot be prevented completely as no insulation material works perfectly. Nevertheless, there are insulation materials which use for example vacuum insulation panels with a thermal conductivity of about $\lambda \leq 0.005 \text{ W m}^{-1} \text{ K}^{-1}$ so that the heat loss can already be minimized. On the left side a heat flux through the wall from the hot (red) to the cold (blue) region is shown. This effect results from the fact, that most TES are made of metal walls which have a much higher thermal diffusivity than most storage mediums. Therefore these walls lead to a thermal bridge between the hot and the cold layers of the stratification.

2 Experimental set-up

2.1 Model experiment

Because of their large dimensions and the absence of any optical access, conventional TES are poorly suited for the investigation of the parasitic flows. For this reason a convection cell was designed which serves as a simplified model of a TES. The convection cell is built as a rectangular polycarbonate tank with a height of 750 mm on a base of $375 \times 375 \text{ mm}^2$. Optionally an aluminium plate can be placed on one side of the tank to work as a thermally high conducting storage wall. Polycarbonate has with $a_{PC} \approx 0.13 \cdot 10^{-6} \text{ m}^2 \text{ s}^{-1}$ nearly the same thermal diffusivity as water while the thermal diffusivity of aluminium $a_{Al} \approx 99 \cdot 10^{-6} \text{ m}^2 \text{ s}^{-1}$ is

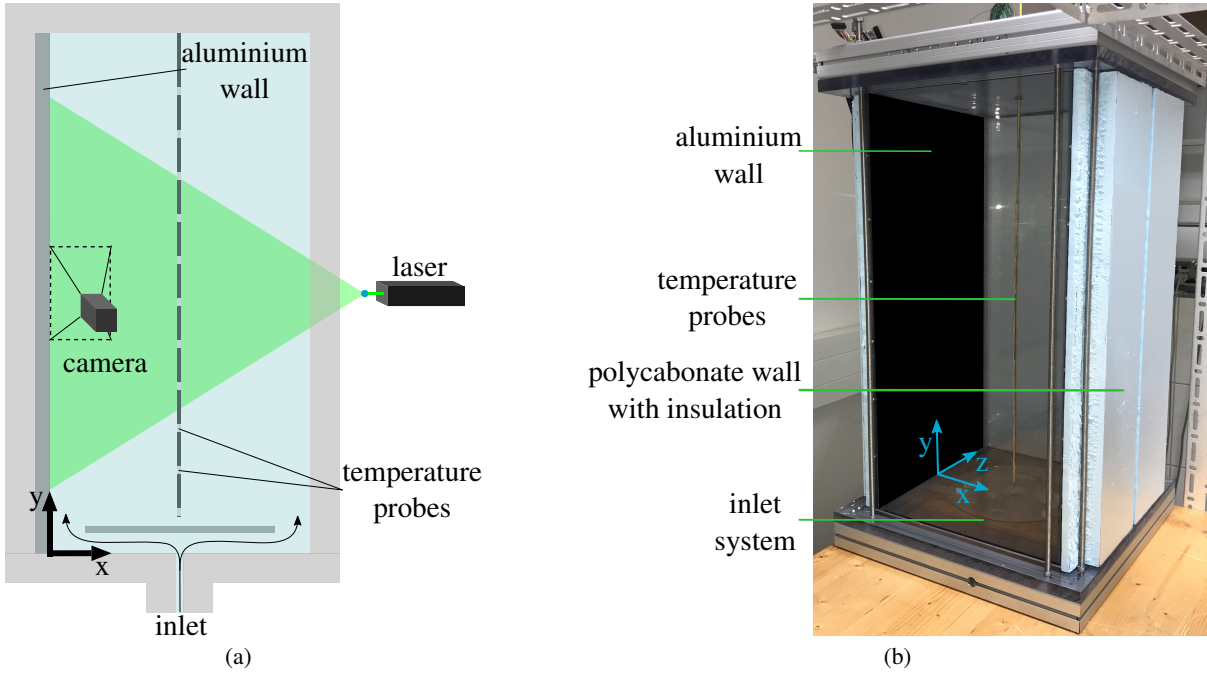


Figure 2: (a) Schematical depiction of the whole measurement set-up including the convection cell with camera and laser for the PIV measurements. (b) Photograph of the insulated convection cell.

two orders of magnitude higher than that of water. Thus thermal diffusion in polycarbonate is as fast as in water without inducing parasitic flow near the wall. The thermal diffusion of aluminium on the other hand is that much higher that the aluminium plate will act as a thermal bridge between the hot and cold layer of water and thus induces vertical convection near the wall. As already mentioned in section 1 the cooling or heating from the environment of the convection cell can also cause undesirable thermal convection in the regions near the wall. Therefore, the whole convection cell is insulated with polystyrene panels to minimize this effect.

To measure the temperatures for the evaluation of the thermal stratification there are temperature probes placed in both, the water and inside the aluminium plate. In the latter 15 PT100 elements are equally distributed over the height. The temperatures in the water are measured by 15 thermocouples which are attached to a thin insulated stainless steel rod. The thermocouples are distributed over the height at the same positions as the PT100 elements in the wall.

The filling of the convection cell is done through an inlet in the bottom plate of the cell. A thin horizontal plate slows the incoming flow down so that there is no free jet which disturbs the stratification inside the cell. Figure 2(a) shows the schematic experimental set-up and figure 2(b) a photograph of the convection cell.

2.2 Validation of the experimental set-up

After its design and construction the convection cell was tested for the achievable thermal stratification. Additionally it was determined whether the aluminium plate has a negative effect on the stratification as expected. For this purpose two measurements were done, one without the aluminium plate and one with the installed aluminium plate. In both cases a stratification was produced under the same conditions and the time series for the temperatures in the water were measured. The results of these measurements are shown in figure 3.

The diagram shows the dimensionless cell height $y^* = y/H$ over the dimensionless temperature $\Theta = (T - T_{min}) / (T_{max} - T_{min})$ for four temperature profiles with each of them consisting of 15 measurement positions of the temperature probes inside the water. To normalize the minimum and maximum temperature T_{min} and T_{max} of all four profiles were taken. The blue profiles show the measurement without the aluminium wall at the times $t = 0h$ and $t = 22h$ while the two orange profiles show the measurement with the installed

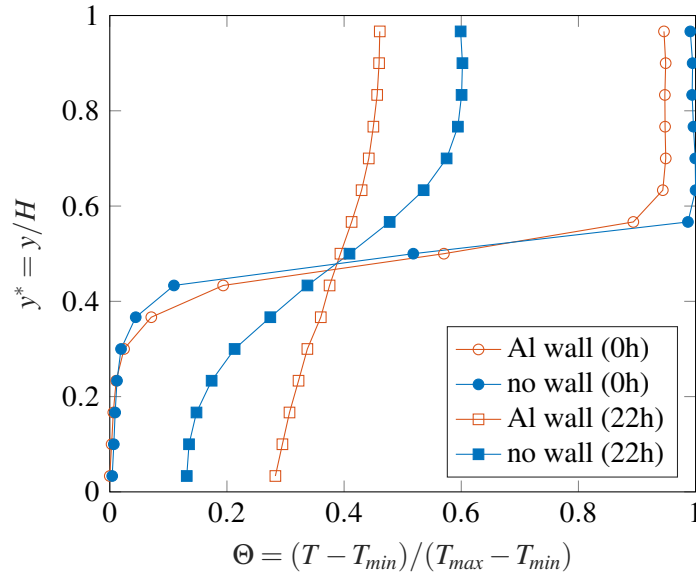


Figure 3: Comparison of the temperature profiles in the convection cell between a measurement with (orange profiles) and without (blue profiles) the aluminium plate inside the cell. Profiles with circles as measuring points show the resulting profiles at the time $t = 0\text{h}$ and with stars marked measuring points show the results at $t = 22\text{h}$.

aluminium wall at the same point in time.

The two profiles at the time $t = 0\text{h}$ show that the generation of a thermal stratification works well as in both cases, with and without aluminium wall, a hot region with homogeneous temperature in the upper 40% of the convection cell and a homogeneous cold region in the lower 30% of the cell exist. Between these regions the temperature gradient rises to a maximum of $\partial T / \partial y = 0.69\text{ K mm}^{-1}$. This zone is called thermocline and in an ideal stratification its thickness would be close to zero.

But even if in both cases the generation of a thermal stratification succeeded the profiles show the influence of the aluminium wall. The highest temperature in the case with installed aluminium wall is only in the region of 90 to 95% of the temperature without the wall. Additionally the temperature gradient in the thermocline is not that high which shows that the aluminium wall conducts the heat from top to bottom.

The two profiles at the time $t = 22\text{h}$ show that in the case without installed wall there are still two regions at the top and the bottom of the cell with homogeneous temperatures. The thermocline of this profile lies in the range between 20 and 80% of the cell height which accompanies with a strongly decreased temperature gradient compared to the profile from the beginning. The other profile shows that the installed aluminium wall accelerates the temperature equalisation so that the thermocline extends over the whole cell height and there are no regions with homogeneous temperature left.

This experiment proves the expected effect of the installed aluminium wall to enhance the heat transfer between the hot and cold layer of the storage medium in a stratified TES.

3 Measuring procedure

During each measurement the temperature of the water decreases and thus the thermal stratification disappears. Therefore a new filling of the cell before each measurement is necessary as the water cannot be heated inside the tank. Between different measurements the water is stored in a barrel besides the cell. This has the advantage of adding the seeding particles to the water before the measurement starts and it is not necessary to seed the water during the filling. Moreover the particles can be reused, which is important for high quality fluorescent tracer particles.

The temperature adjustment of the water for the hot and the cold region of the stratification is done by cooling the water inside the barrel and heating it on its way to the convection cell during the filling process. A thermostat is used to cool the water down to a minimum temperature of about 7°C . Between the barrel and the convection cell a pump is installed to carry the water inside the cell. This can be done

through two different pipelines of which one has a flow heater installed to heat the water for the hot part of the stratification. The maximum temperature that can be achieved by the flow heater is about 60°C. The temperatures of the water flowing through the pipeline is measured before it enters the convection cell.

To start the filling the pump is turned on and the water is routed through the pipeline with the flow heater. If half of the convection cell is filled with hot water the following water is routed through the other pipeline and the bottom half gets filled directly with the cooled water from the barrel. During the filling process, a mixing of the hot and the cold water has to be prevented. For this purpose the volume flow rate is decreased between the filling of the hot and the cold water so that the hot water streams in with a flow rate of 2.6 l min⁻¹ and the cold water streams in with 1.5 l min⁻¹. After finishing the filling process five minutes are waited before starting the Particle Image Velocimetry (PIV) measurements to let the flow calm down.

To perform the PIV measurements a laser and a camera are arranged in a 90 degree angle (as schematically shown in figure 2(a)). The sCMOS camera has a sensor size of 2560 × 2160 px and a pixel size of 6.5 × 6.5 μm². A lens with a focal length of 100 mm and a minimal f-number of f/1.4 is used to measure velocities near the aluminium wall. The obtained field of view has a size of about 41 × 35 mm² with a resolution of 62 px mm⁻¹. For illumination a Nd:YAG double pulse laser with a wave length of 532 nm and a pulse energy of about 20 mJ per pulse is used to form a light sheet. Due to the low velocities the measurements are done in single frame mode at 5 Hz repetition rate.

After finishing a measurement the water is drained back to the barrel. There it gets cooled again until the minimum temperature for the next measurement is reached. After this the whole process can be started again.

4 Results and discussion

Figure 4 shows the results of three PIV measurements near the aluminium wall at different heights. The measurement in figure 4(b) was performed in the regions of the thermocline at half of the cell height ($y = 375$ mm), the two other measurements were done 120 mm below (figure 4(a)) and 120 mm above (figure 4(c)) the thermocline. Each of the measurement was carried out as described in section 3.

The measured inlet temperatures for each measurement were between 58 and 60°C for the hot layers and between 6 and 7°C for the cold layers. The water temperatures measured inside the cell are between 52 and 53°C in the hot layer and 9 and 11°C in the cold layer for all measurements. The differences between the inlet temperatures and the measured temperatures inside the cell resulted from the fact that the convection cell had room temperature before the filling. Therefore the hot water heats the whole cell and the aluminium wall during the filling process and after that the cold water cools the cell and the aluminium wall. Differences in the measured stratification temperatures may result from different room temperatures as the measurements were not performed at the same day.

The evaluation of the figures 4(a) and 4(b) were made by averaging 499 the vector fields of 500 images with a time difference of $\Delta t = 0.2$ s. The resolution of calculated vector fields amounts 12 × 12 px. Figure 4(c) shows an averaged vector field of 9000 images with the same difference in time of $\Delta t = 0.2$ s. Before they got averaged effectively instantaneous vector fields were calculated by using the pyramid sum of correlation algorithm with Gaussian weighting. This algorithm uses the sum of correlation technique with the additional approach to correlate not only two consecutive images but also for example the first and the third image. This leads to the fact that slow as well as fast velocities in the measuring zone can be evaluated. In this case the algorithm was used for five images in each case, so that the time averaging of this technique was small in comparison to the time in which the flow field changes. Due to this time averaging the spatial resolution could be increased to 8 × 8 px [Kähler et al. (2012a)].

The results show an upward directed convection flow on the wall in the lowest measurement position (figure 4(a)). The fluid in this region gets heated by the heat flux through the aluminium wall which leads to a decreased density and thus to an acceleration upwards. The layer thickness is in a range of about 4 to 5 mm and the amplitude of this flow is up to 2.5 mm s⁻¹.

In the upper part of the cell (figure 4(c)) the vertical convection is downward directed due to the heat flux from the fluid to the aluminium wall in this region. The layer thickness is about 3 to 4 mm which is less than it is in the lower region. One explanation for this could be that the decreased viscosity due to the higher water temperatures decreases the shear stress between different fluid particles and the boundary layer gets thinner. Due to this decreased shear stress the convective flow in the hot region of the cell is faster than it is in the cold region. This can be seen in the contour plot that shows that the amplitude of the flow is up to 4 mm s⁻¹.

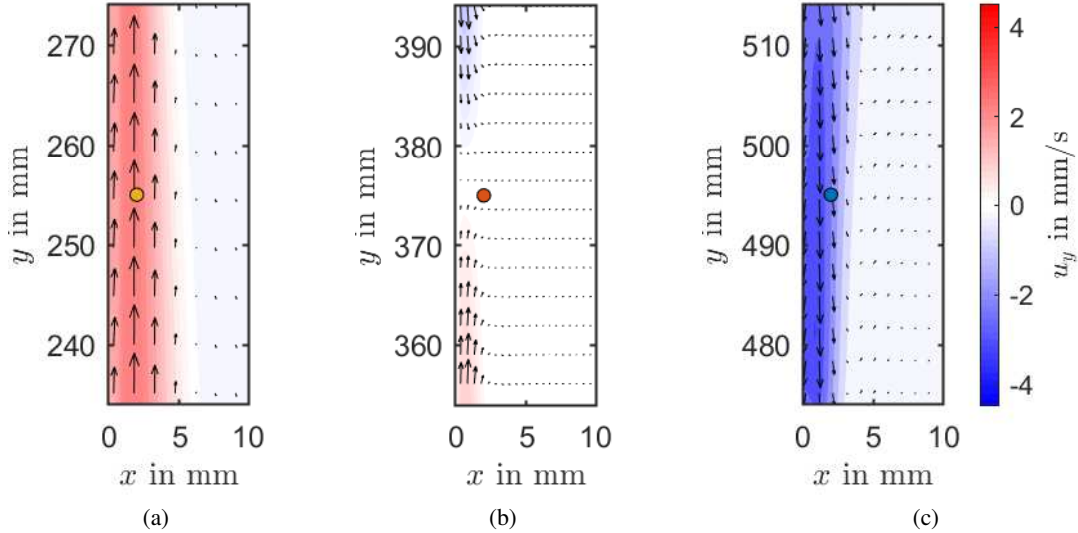


Figure 4: Averaged PIV measurements near the aluminium wall of the convection cell. For each measurement position a separate filling was made. Every measurement started five minutes after finishing the filling to still induced flow of the filling process. (a) Upward directed vertical flow in the cold region (120 mm below the thermocline). (b) Approaching counter directed vertical flows at half of the tank height ($y^* = 0.5$). (c) Downward directed vertical flow in the hot region (120 mm above the thermocline). The vector arrows show the flow direction, the value of the vertical velocity component is shown by the contour plot.

In the middle part of the convection cell (figure 4(b)) the two vertical convection flows approach and thus slow down each other. In this process the two flows are redirected in horizontal direction. The thickness of both boundary layer flows decreases in this region and is in a range of 1 to 2mm. To investigate these three flows in a more detailed way their temporal progression is compared in figure 5.

The diagram shows the temporal development of the velocity magnitude in different heights. The orange line shows the velocity in the middle of the thermocline which is due to the approaching vertical flows very slow. There are some small fluctuations with in this time series with a standard deviation of 0.06 mm s^{-1} but overall the velocity can be denoted as nearly constant.

The yellow line shows the time series of the velocity in the cold region of the convection cell. Similar to the velocity in the thermocline there are only little fluctuations in the velocity which are small compared to the magnitude. Moreover the graph shows a small decrease in the magnitude over time. This results from the overall cooling of the system.

But the largest fluctuations can be seen in the hot region in a height of $y = 495 \text{ mm}$. It shows huge fluctuations which are in the order of magnitude of the average velocity in this area. The reason for this behaviour could be the same as for the smaller and faster flows in the boundary layer. The lower viscosity of the hot water enables the faster flow which seems to be in transition to turbulence in this region.

5 Conclusion

An experimental set-up for the investigation of parasitic thermal convection in stratified thermal energy storages was designed and the negative effect of a high heat conducting storage wall was proven. PIV measurements near this wall were realized. Time averaged vector fields at three different positions in height showed two thermal convection flows on this wall. In the lower part, where the cold water is positioned, the water gets heated by a heat flux from the wall. This leads to upward directed thermal convection near the wall. In the upper part of the experiment a second thermal convection flow forms itself due to the heat flux from the hot water to the storage wall which cools the water in the near-wall region. At the height $y^* = 0.5$ these two flows approach, slow down each other and get redirected in horizontal direction.

In each of these three measurement positions a time series of the velocity in one point of the flow field near the wall was evaluated. The temporal developments at these three points show that the flows in the

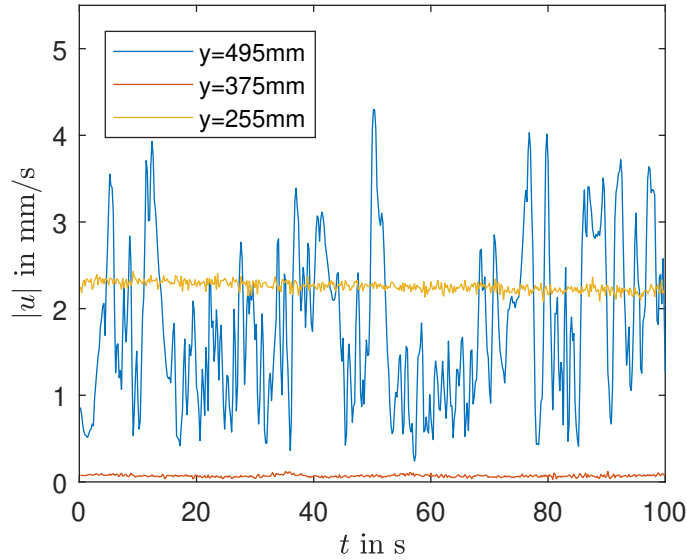


Figure 5: Temporal development of the velocity magnitude in the first 100s of the three PIV measurements shown in figure 4. Each graph is measured at a horizontal distance to the wall of $x = 2$ mm. The vertical positions vary from $y = 255$ mm over $y = 375$ mm to $y = 495$ mm.

lower and middle part of the convection cell are rather stable in time without huge fluctuations. In contrast to this the velocity in the upper part underlies big variations which are in the order of magnitude of its average value.

For future research fluorescent particles in combination with a notch filter will be used to disturb reflections of the light sheet on the aluminium wall and thus improve the measurements. Moreover Particle Tracking Velocimetry (PTV) will be used which is more reliable for measurements near the wall [Kähler et al. (2012b)].

Acknowledgements

This research was supported by the European Regional Development Fund (ERDF) in cooperation with the Thüringer Aufbaubank (2017 FE 9086).

References

- Kähler CJ, Scharnowski S, and Cierpka C (2012a) On the resolution limit of digital particle image velocimetry. *Experiments in Fluids* 52:1629–1639
- Kähler CJ, Scharnowski S, and Cierpka C (2012b) On the uncertainty of digital PIV and PTV near walls. *Experiments in Fluids* 52:1641–1656
- Thess A (2013) Thermodynamic Efficiency of Pumped Heat Electricity Storage. *Phys Rev Lett* 111:110602